frontiers in Materials

ORIGINAL RESEARCH
published: 16 November 2020
doi: 10.3389/fmats.2020.593345

High Performance Dye-Sensitized Solar Cells Based on Electrospun MoS_2-Carbon Nanofiber Composite Counter Electrode

Hengchao Sun, Xianzi Zhou*, Wen Yang, Yang Gao, Ruopu Zhang, Jianjun Liu, Haibao Wang, Yan Guo and Zheng Wang*

Beijing Smart-Chip Microelectronics Technology Co., Ltd., Beijing, China

MoS_2-carbon nanofiber composites were prepared *via* electrospun technique with ammonium thiomolybdate(VI) and polyvinylpyrrolidone. The effects of thermal pretreatment on the morphology of material were studied. The results demonstrate that the composite nanofiber with pretreatment shows a uniform diameter and lots of small size MoS_2 particles inside with porous structure. When the composites was used as counter electrodes in dye-sensitized solar cell, a maximum efficiency of 5.7% has been achieved due to the combination of electrical conductivity and catalysis ability from MoS_2-carbon nanofiber composites.

Keywords: dye-sensitized solar cell, counter electrode, MoS_2, carbon nanofiber, composite material, electrospun

OPEN ACCESS

Edited by:
Jinliang Li,
Jinan University, China

Reviewed by:
Tongtong Xuan,
Xiamen University, China
Yong Liu,
Qingdao University of Science and Technology, China

****Correspondence:***
Xianzi Zhou
zhouxianzi@sgitg.sgcc.com.cn
Hengchao Sun
sunhengchao@sgitg.sgcc.com.cn

Specialty section:
This article was submitted to Energy Materials, a section of the journal Frontiers in Materials

Received: *10 August 2020*
Accepted: *03 September 2020*
Published: *16 November 2020*

Citation:
Sun H, Zhou X, Yang W, Gao Y, Zhang R, Liu J, Wang H, Guo Y and Wang Z (2020) High Performance Dye-Sensitized Solar Cells Based on Electrospun MoS_2-Carbon Nanofiber Composite Counter Electrode. Front. Mater. 7:593345. doi: 10.3389/fmats.2020.593345

INTRODUCTION

For nearly thirty years, due to the advantages of low price and simple preparation, a lot of attention has been paid to dye sensitized solar cells (DSSCs) (Sun et al., 2015; Sun et al., 2020). In a typical DSSC with sandwich structure, electrons excite from the dye and inject to the conduction band of the photoanode, then the oxidized dye could be reduced by a charge mediator in electrolyte (Miao et al., 2015). Counter electrode plays an important role in this process, which take charge of reducing I_3^- to I^- in electrolyte and collecting electrons from external circuit (Yue et al., 2014; Yun et al., 2014). Although, the traditional Pt counter electrode has an outstanding catalytic performance, its high price and poor corrosion resistance seriously hinder its mass production process. Therefore, it is of great significance to develop new materials instead of Pt counter electrode (Hauch and Georg, 2001; Olsen et al., 2000).

Benefit from the uniform radial structure and good transmission characteristics, one-dimensional carbon materials are superior to other carbon materials in electrical conductivity (Ramasamy et al., 2008; Poudel and Qiao, 2012; Kim and Yong, 2013). Recently, carbon nanofibers, carbon nanotubes, carbon nanowires with porous structure have been widely used in the DSSCs, secondary batteries or other energy fields (Li et al., 2019; Pan et al., 2019; Jia et al., 2020; Pan et al., 2020; Qin et al., 2020; Yuan et al., 2020; Zhu et al., 2021). Joshi et al. prepared carbon nanofiber counter electrode through electrospinning for DSSC, which obtained an efficiency of 5.5% (Zhu et al., 2010). Zou et al. made an one-dimensional DSSC using carbon fiber as counter electrode, with an efficiency of 2.7% (Hou et al., 2011). Guo et al. synthesized Pt-carbon fiber composite counter electrode to obtain a high efficiency of 8.97% (Zhang et al., 2015). Xiao et al. used single-walled carbon nanotubes combined with Pt as counter electrode, through optimizing the content of carbon nanotubes, with an efficiency of 5.96% (Ruan et al., 2011).

In our previous work, MoS_2-nitrogen doped carbon shell-core microspheres have been synthesized for Pt-free DSSC (Zhu et al., 2017). Thus it can be expected that MoS_2-carbon nanofiber composites should be promising counter electrode materials for DSSCs. In this work, a simple and fast electrospinning method was employed to synthesize MoS_2-carbon nanofiber composites. After thermal treatment, the composites material were used as counter electrodes of DSSCs, with an efficiency of 5.7% under 1 sun illumination.

EXPERIMENTAL

Preparing Composites Material and Counter Electrode

In a typical process, a certain amount of ammonium thiomolybdate(VI) (0.2 M) and polyvinylpyrrolidone (1,300,000 g/mol) (8 wt%) were dissolved in N, N-dimethylformamide. The solution was then placed into a needle. The applied voltage was 20 kV, and the distance between the needle and the stainless steel roller was 15 cm. The flow rate was set as 0.6 ml/h. Subsequently, the samples were separated into two parts. One thermally treated at 800°C for 2 h in an N_2/H_2 atmosphere, named as mesoporous silica nanofiber (MSF). For the other part, a pretreatment process is added before thermal treatment, which is kept in air atmosphere at 280°C for 2 h with a heating rate 2°C min^{-1}, and named as air-MSF. The as-synthesized composites material were coated onto the cleaned F-doped SnO_2 (resistivity: 14 Ω/□, Nippon Sheet Glass, Japan) glass using the screen printing method, and were annealed at 400°C for 30 min, then used as counter electrodes. The mass of the activated material is ~5 mg in one counter electrode. The conventional Pt film and pure MoS_2 film were also used as counter electrodes for comparison.

Preparing Dye Sensitized Solar Cells

The photoanodes were prepared of P25 paste on F-doped SnO_2 glass by screen printing method. After sintered at 450°C for 30 min and cooled to 80°C, photoanodes were immersed into 0.5 mM N719 dye solution for 24 h. The redox electrolyte contained of 0.6 M 1-butyl-3-methylimidazolium iodide, 30 mM I_2, 0.5 M *tert*-butylpyridine, and 0.1 M guanidinium thiocyanate in a solvent mixture of 85% acetonitrile with 15%

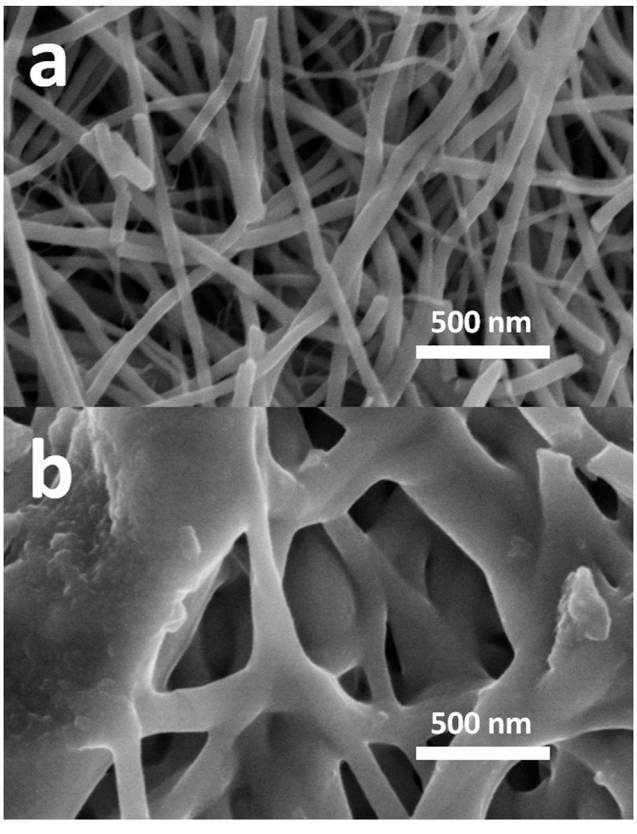

FIGURE 1 | Field emission scanning electron microscope images of **(A)** air-mesoporous silica nanofiber and **(B)** mesoporous silica nanofiber.

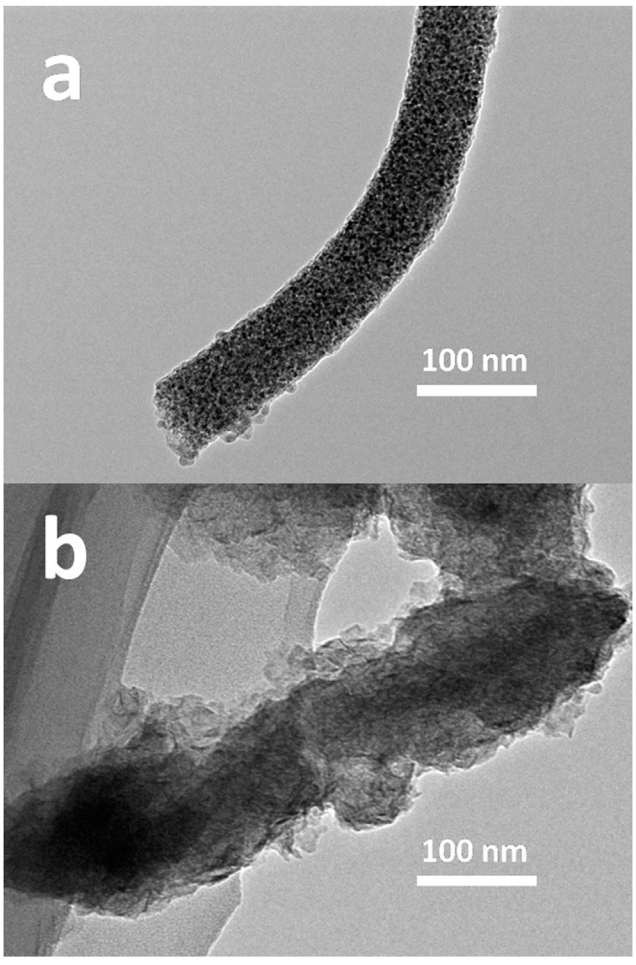

FIGURE 2 | Low-magnification transmission electron microscope images of **(A)** air-mesoporous silica nanofiber and **(B)** mesoporous silica nanofiber.

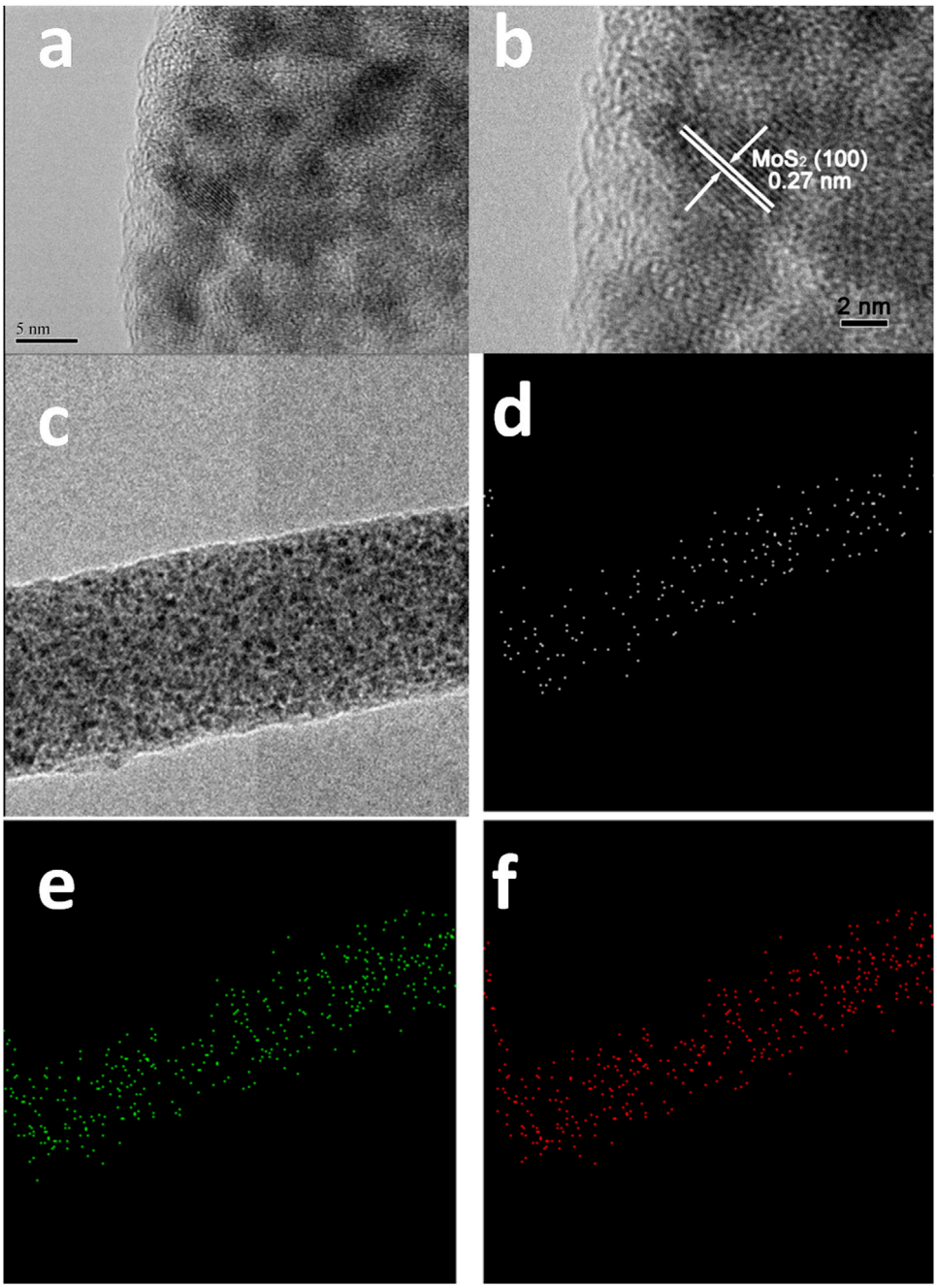

FIGURE 3 | High-magnification transmission electron microscope images of **(A)**; **(B)** air-mesoporous silica nanofiber; **(C)**–**(F)** element mapping of air-mesoporous silica nanofiber; the white points in **(D)** for C; the green points in **(E)** for S; the red points in **(F)** for Mo.

valeronitrile by volume. The photoanodes and counter electrodes were sealed together with a 60 μm spacer (Surlyn), with an active area of 0.2 cm^2.

Characterization

The morphology and structure of the samples were analyzed by field emission scanning electron microscope (FESEM, JEOL JSM-LV5610), transmission electron microscope (TEM, JeOL-2010) and X-ray diffractometer (XRD, Holland Analytical PRO PW3040/60) using copper target Kα radiation (V = 30 kV, I = 25 mA, λ = 1.5418 Å). The cyclic voltammetry (CV) curve and electrochemical impedance spectra were characterized with a three-electrode system by an electrochemical workstation (Autolab PGSTAT 302N). The photocurrent density–photovoltage curves (J–V) were measured by the NewPort solar simulator system equipped with a digital source meter (Keithley 2440), at 1 sun (AM 1.5 G, 100 mW cm^{-2}).

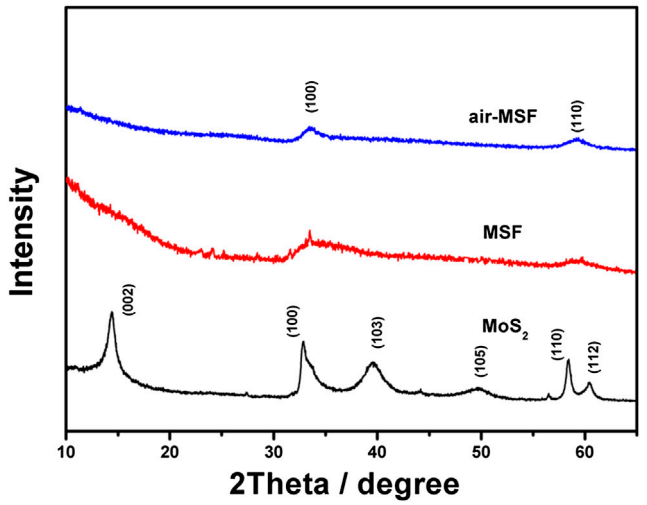

FIGURE 4 | X-ray diffractometer patterns of air-mesoporous silica nanofiber (MSF), MSF, and MoS_2.

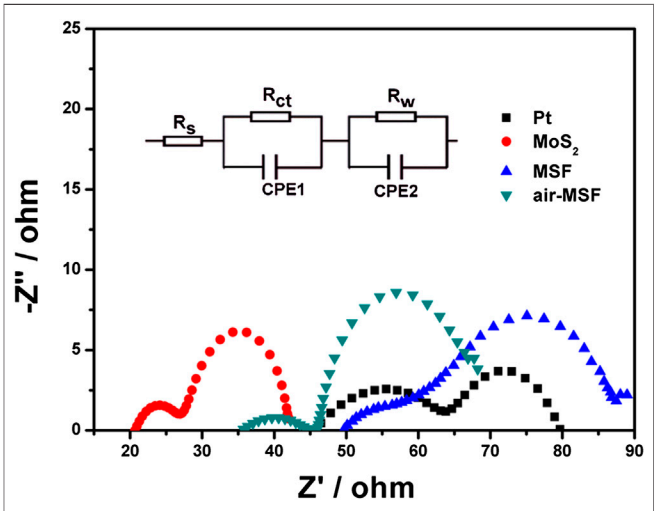

FIGURE 6 | Electrochemical impedance spectra of DSSCs with air-mesoporous silica nanofiber (MSF), MSF, MoS_2, and Pt counter electrodes. Inset displays the corresponding equivalent circuit.

RESULTS AND DISCUSSION

The FESEM of air-MSF with pretreatment are shown in **Figure 1A**. As illustrated in **Figure 1A**, a large number of one-dimensional carbon nanofiber are interactively connected together, forming a three-dimensional network structure, which is conducive to the transmission of electrons. **Figure 1B** shows FESEM image of MSF. It can be observed that MSF has serious adhesion, bulky fiber and is not separable, which is not conducive to electron transmission.

The detailed morphologies of air-MSF and MSF are shown by TEM in **Figure 2**. It can be clearly seen from **Figure 2A** that the carbon nanofiber of air-MSF are uniform in thickness along the axial direction, with a diameter of about 50 nm. A large number of uniformly distributed black spots in the fiber are MoS_2 particles. The nanofiber of MSF shown in **Figure 2B** are short and thick and uneven in diameter due to adhesion (Zhu et al., 2010).

Figures 3A,B are high-magnification TEM images of air-MSF. It can be found from **Figure 3A** that a large number of MoS_2 nanoparticles are uniformly distributed in the carbon nanofiber. In the further enlarged **Figure 3B**, the lattice fringes with interplanar spacing of 0.27 nm correspond to the (100) crystal plane of hexagonal MoS_2. **Figures 3C–F** are the element distribution diagrams of air-MSF, where the white dots in **Figure 3D** are carbon elements, the green dots in **Figure 3E** are sulfur, and the red dots in **Figure 3F** are molybdenum. The distribution diagram can illustrate that a large number of MoS_2 nanoparticles are uniformly distributed in the carbon nanofiber.

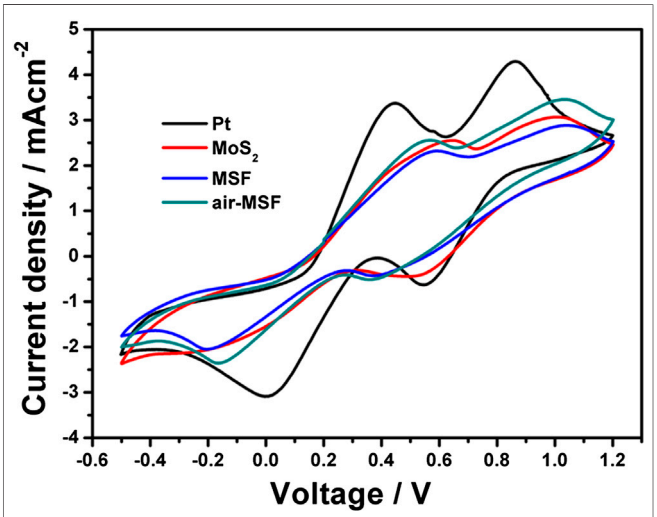

FIGURE 5 | Cyclic voltammetry curves of air-mesoporous silica nanofiber (MSF), MSF, MoS_2, and Pt electrodes.

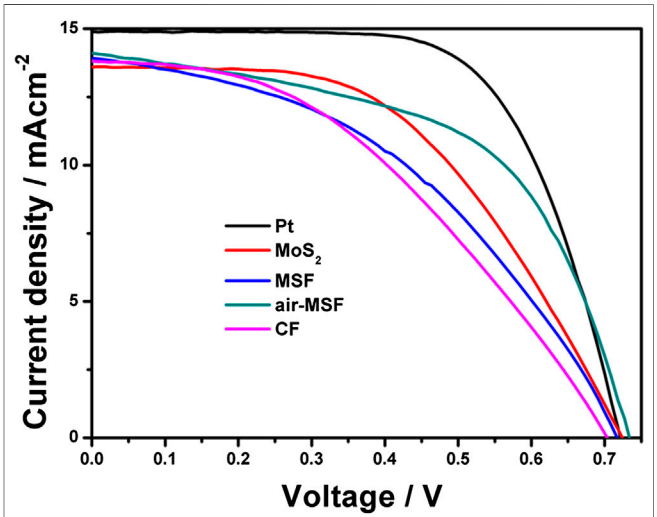

FIGURE 7 | *J–V* curves of dye sensitized solar cells with air-mesoporous silica nanofiber (MSF), MSF, CF, MoS_2, and Pt counter electrodes.

The XRD patterns of air-MSF, MSF and pure MoS_2 prepared by microwave methods are shown in **Figure 4**. Both air-MSF and MSF have diffraction peaks near ~33.5° and ~68°, corresponding to the (100) hexagonal crystal form of MoS_2, which is consistent with the (110) crystal plane and the PDF card (JCPDS card no.73-1508). It shows that the pretreatment does not affect the formation of MoS_2 crystals. However, the XRD patterns of the MoS_2 crystal synthesized by electrospun and the MoS_2 crystal prepared by the microwave method are not exactly the same. Smaller MoS_2 crystals through electrospun grow preferentially in a specific direction, with low crystallinity and disordered structure. Due to the low carbon content in the two composite samples, the C (002) peak around ~26° is relatively weak (Qin et al., 2015).

The electrochemical performance of air-MSF, MSF, MoS_2 and Pt electrodes are shown by CV curves in **Figure 5**. Although both composite electrodes show catalytic ability to iodine-based electrolyte, the peak current density of MSF electrode is very close to or even lower than MoS_2, which indicates that the electrochemical catalytic capacity of MSF without pretreatment has not been enhanced. It should be resulted by excessive adhesion of carbon nanofiber with weak conductivity. The current density of the pretreated air-MSF has been improved, which shows that the carbon nanofiber composite MoS_2 electrode has a higher catalytic ability to iodine-based electrolyte than the MoS_2 electrode. This is because the carbon nanofiber network is conducive to the transmission of electrons. Combined with the catalytic ability of MoS_2, air-MSF electrode with stronger performance is obtained (Li et al., 2010; Wang et al., 2011).

Figure 6 shows the Nyquist spectrum of the four electrodes, and the inset shows its equivalent circuit. A typical electrochemical impedance spectra curve of a DSSC has two semicircles. The large semicircle in the low frequency region corresponds to the reaction at the photoanode/electrolyte interface reaction, and the small semicircle in the high frequency region corresponds to the reaction on counter electrode/electrolyte. So the high-frequency semicircle is the focus of characterizing the performance of the counter electrode. According to the equivalent circuit, R_s is the series resistance of the cell. R_{ct} is the charge transfer resistance at the counter electrode/electrolyte interface. And R_w is the charge transfer resistance at the photoanode/electrolyte interface. It can be seen from the fitting that the R_{ct} value (25.9 Ω) of the MSF counter electrode is higher than the MoS_2 counter electrode (22.3 Ω), which indicates that the MSF counter electrode does not perform well, which is consistent with the CV results. The R_{ct} value of the air-MSF counter electrode is about 16.6 Ω, significantly lower than MoS_2, which indicates that the electrochemical performance of the pretreated carbon nanofiber composite MoS_2 counter electrode is better than that of the pure MoS_2 counter electrode (Rick et al., 2014).

Figure 7 shows *J–V* curves of DSSCs based on composite counter electrodes, pure carbon nanofiber, pure MoS_2, and traditional Pt counter electrode. Comparing the current density (J_{sc}), open circuit voltage (V_{oc}), fill factor (FF) and conversion efficiency (η) of pure carbon nanofiber and pure MoS_2 counter electrode (as shown in **Table 1**), it can be found that MSF with severe adhesion of carbon nanofiber has a lower FF (43.3%) and η (4.4%) than the pure MoS_2 counter electrode (50.8%, 5.0%), and only slightly higher than the pure carbon nanofiber counter electrode (41.5%, 4.2%). The pre-processed air-MSF counter electrode exhibits more impressive photovoltaic performance, with FF and η reaching 55.0 and 5.7%, respectively, which are higher than the one-dimensional DSSC made by Zou (Hou et al., 2011). This shows that the pre-heat treatment of carbon nanofiber is beneficial to the morphology of the sample, thereby improving the conductivity of the sample. Moreover, the comparison with the pure MoS_2 counter electrode shows that the combination of carbon nanofiber and MoS_2 benefits from the close adhesion, which can combine the excellent electrical conductivity of carbon nanofiber with the good catalytic ability of MoS_2 to obtain a composite electrode with better performance. Although the air-MSF electrode does not exceed the Pt counter electrode in photovoltaic performance, the simpler and faster method of electrospinning will benefit the industrial production of DSSCs (Wang et al., 2011).

TABLE 1 | Photovoltaic parameters of the cells with air-mesoporous silica nanofiber (MSF), MSF, CF, MoS_2, and Pt counter electrodes.

Sample	J_{sc} (mA cm^{-2})	V_{oc} (V)	FF (%)	η (%)
MoS_2	13.6	0.72	50.8	5.0
MSF	13.9	0.71	43.3	4.4
Air-MSF	14.1	0.73	55.0	5.7
CF	13.8	0.70	41.5	4.2
Pt	14.9	0.72	65.2	7.0

CONCLUSION

The electrospinning method is used to prepare carbon nanofiber and MoS_2 composite material with ammonium tetrathiomolybdate and polyvinylpyrrolidone as raw materials. Through characterization, it is found that the MoS_2 particles synthesized by this method are small in size and densely distributed among the carbon nanofiber. The influence of the pretreatment on the formation of carbon nanofiber was discussed. Through the comparison of several kinds of electrodes, it can be found that the efficiency of the pretreated air-MSF composite counter electrode can reach 5.7%, which is higher than that of pure carbon nanofiber and pure MoS_2 counter electrode.

DATA AVAILABILITY STATEMENT

All datasets presented in this study are included in the article.

AUTHOR CONTRIBUTIONS

HS and XZ proposed ideas and wrote papers. Experiment was done by HS. WY, YG, RZ, and JL modified articles. HW, YG, and ZW provided financial and technical support.

FUNDING

The authors declare that this study received funding from 2020 State Grid Corporation Headquarters Technical Service (546816200012). The funder was not involved in the study design, collection, analysis, interpretation of data, the writing of this article or the decision to submit it for publication.

REFERENCES

Hauch, A., and Georg, A. (2001). Diffusion in the electrolyte and charge-transfer reaction at the platinum electrode in dye-sensitized solar cells. *Electrochim. Acta* 46 (22), 3457–3466. doi:10.1016/S0013-4686(01)00540-0

Hou, S., Cai, X., Fu, Y., Lv, Z., Wang, D., Wu, H., et al. (2011). Transparent conductive oxide-less, flexible, and highly efficient dye-sensitized solar cells with commercialized carbon fiber as the counter electrode. *J. Mater. Chem.* 21 (36), 13776–13779. doi:10.1039/c1jm12056e

Jia, N., Qin, W., Wu, C., and Jia, C. (2020). Graphene-attached vanadium sulfide composite prepared *via* microwave-assisted hydrothermal method for high performance lithium ion batteries. *J. Alloys Compd.* 834, 155073. doi:10.1016/j.jallcom.2020.155073

Kim, H., and Yong, K. (2013). A highly efficient light capturing 2D (nanosheet)-1D (nanorod) combined hierarchical ZnO nanostructure for efficient quantum dot sensitized solar cells. *Phys. Chem. Chem. Phys.* 15, 2109. doi:10.1039/c2cp44045h

Li, G-R., Wang, F., Jiang, Q-W., Gao, X-P., and Shen, P-W. (2010). Carbon nanotubes with titanium nitride as a low-cost counter-electrode material for dye-sensitized solar cells. *Angew. Chem. Int. Ed.* 49 (21), 3653–3658. doi:10.1002/anie.201000659

Li, J., Zhuang, N., Xie, J., Zhu, Y., Lai, H., Qin, W., et al. (2019). Carboxymethyl cellulose binder greatly stabilizes porous hollow carbon submicrospheres in capacitive K-ion storage. *ACS Appl. Mater. Interfaces* 11, 15581. doi:10.1021/acsami.9b02060

Miao, C., Chen, C., Dai, Q., Xu, L., and Song, H. (2015). Dysprosium, Holmium and Erbium ions doped Indium Oxide nanotubes as photoanodes for dye sensitized solar cells and improved device performance. *J. Colloid Interface Sci.* 440 (0), 162–167. doi:10.1016/j.jcis.2014.10.055

Olsen, E., Hagen, G., and Eric Lindquist, S. (2000). Dissolution of platinum in methoxy propionitrile containing LiI/I_2. *Sol. Energy Mater. Sol. Cell.* 63 (3), 267–273. doi:10.1016/S0927-0248(00)00033-7

Pan, W., Li, J., Liu, X., Zhou, N., Wu, C., Ding, M., et al. (2019). Formation of needle-like porous $CoNi_2S_4$-MnOOH for high performance hybrid supercapacitors with high energy density. *J. Colloid Interface Sci.* 554, 125–132. doi:10.1016/j.jcis.2019.07.010

Pan, Y., Zhang, Y., Zhang, Y., Zhang, Q., Gao, X., Dou, X., et al. (2020). MoC nanoparticle-embedded carbon nanofiber aerogels as flow-through electrodes for highly efficient pseudocapacitive deionization. *J. Mater. Chem.* 8 (3), 1443–1450. doi:10.1039/C9TA11537D

Poudel, P., and Qiao, Q. (2012). One dimensional nanostructure/nanoparticle composites as photoanodes for dye-sensitized solar cells. *Nanoscale* 4 (9), 2826–2838. doi:10.1039/c2nr30347g

Qin, W., Chen, T., Pan, L., Niu, L., Hu, B., Li, D., et al. (2015). MoS_2-reduced graphene oxide composites via microwave assisted synthesis for sodium ion battery anode with improved capacity and cycling performance. *Electrochim. Acta* 153, 55–61. doi:10.1016/j.electacta.2014.11.034

Qin, W., Zhou, N., Wu, C., Xie, M., Sun, H., Guo, Y., et al. (2020). Mini-review on the redox additives in aqueous electrolyte for high performance supercapacitors. *ACS Omega* 5 (8), 3801–3808. doi:10.1021/acsomega.9b04063

Ramasamy, E., Lee, W. J., Lee, D. Y., and Song, J. S. (2008). Spray coated multi-wall carbon nanotube counter electrode for tri-iodide (I_3^-) reduction in dye-sensitized solar cells. *Electrochem. Commun.* 10 (7), 1087–1089. doi:10.1016/j.elecom.2008.05.013

Rick, H., Pan, L., Zhu, G., Piao, X., Zhang, L., and Sun, Z. (2014). Long afterglow $Sr_4Al_{14}O_{25}$:Eu, Dy phosphors as both scattering and down converting layer for CdS quantum dot-sensitized solar cells. *Dalton Trans.* 43 (40), 14936–14941. doi:10.1039/C4DT01276C

Ruan, Y., Wu, J., Yue, G., Lin, J., Huang, M., and Lan, Z. (2011). Low temperature preparation of a high performance Pt/SWCNT counter electrode for flexible dye-sensitized solar cells. *Electrochim. Acta* 56 (24), 8545–8550. doi:10.1016/j.electacta.2011.07.043

Sun, H., Chen, T., Liu, Y., Hou, X., Zhang, L., Zhu, G., et al. (2015). Carbon microspheres via microwave-assisted synthesis as counter electrodes of dye-sensitized solar cells. *J. Colloid Interface Sci.* 445, 326–329. doi:10.1016/j.jcis.2015.01.016

Sun, S., Sartape, R., and Chakraborty, J. (2020). Role of dye-induced corrosion in determining the efficiency of ZnO-based DSSC: the case of ZnO nanoforest in N719. *J. Mater. Sci. Mater. Electron.* 31 (7), 2202. doi:10.1007/s10854-019-02752-5

Wang, H.-Y., Wang, F.-M., Wang, Y.-Y., Wan, C.-C., Hwang, B.-J., and Santhanam, R., et al. (2011). Electrochemical formation of Pt nanoparticles on multiwalled carbon nanotubes: useful for fabricating electrodes for use in dye-sensitized solar cells. *J. Phys. Chem. C* 115 (16), 8439–8446. doi:10.1021/jp201220t

Yuan, Y., Gao, X., Wang, K., Dou, X., Zhu, H., Yuan, X., et al. (2020). Rocking-chair capacitive deionization with flow-through electrodes. *J. Mater. Chem.* 8 (17), 8476–8484. doi:10.1039/C9TA14112J

Yue, G., Ma, X., Jiang, Q., Tan, F., Wu, J., Chen, C., et al. (2014). PEDOT:PSS and glucose assisted preparation of molybdenum disulfide/single-wall carbon nanotubes counter electrode and served in dye-sensitized solar cells. *Electrochim. Acta* 142, 68–75. doi:10.1016/j.electacta.2014.07.107

Yun, S., Hagfeldt, A., and Ma, T. (2014). Pt-free counter electrode for dye-sensitized solar cells with high efficiency. *Adv. Mater.* 26 (36), 6210–6237. doi:10.1002/adma.201402056

Zhang, H., Zhu, Y., Li, W., Zheng, H., Wu, K., Ding, K., et al. (2015). Synthesis of highly effective Pt/carbon fiber composite counter electrode catalyst for dye-sensitized solar cells. *Electrochim. Acta* 176, 997–1000. doi:10.1016/j.electacta.2015.07.103

Zhu, P., Zhang, L., Chen, Q., Galipeau, D., Fong, H., Qiao, Q., et al. (2010). Electrospun carbon nanofibers as low-cost counter electrode for dye-sensitized solar cells. *ACS Appl. Mater. Interfaces* 2 (12), 3572–3577. doi:10.1021/am100742s

Zhu, G., Xu, H., Wang, H., Wang, W., Zhang, Q., Li, Z., et al. (2017). Microwave assisted synthesis of MoS_2/nitrogen-doped carbon shell–core microspheres for Pt-free dye-sensitized solar cells. *RSC Adv.* 7. doi:10.1039/C6RA28850B

Zhu, Y., Gao, X., Wang, Z., Wang, K., Dou, X., Zhu, H., et al. (2021). Controlled synthesis of bismuth oxychloride-carbon nanofiber hybrid materials as highly efficient electrodes for rocking-chair capacitive deionization. *Chem. Eng. J.* 403, 126326. doi:10.1016/j.cej.2020.126326

Conflict of Interest: HS, XZ, WY, YG, RZ, JL, HW, YG, and ZW are employed by Beijing Smart-Chip Microelectronics Technology Co., Ltd.